Nuclear Engineering and Technology 48 (2016) 758–764

Available online at ScienceDirect

Nuclear Engineering and Technology

journal homepage: www.elsevier.com/locate/net

Original Article

The Studies of Irradiation Hardening of Stainless Steel Reactor Internals under Proton and Xenon Irradiation

Chaoliang Xu[*], *Lu Zhang*, *Wangjie Qian*, *Jinna Mei*, *and Xiangbing Liu*

Suzhou Nuclear Power Research Institute, No. 158, Xihuan Road, Gusu district, Suzhou, Jiangsu Province 215004, China

ARTICLE INFO

Article history:
Received 22 September 2015
Received in revised form
7 January 2016
Accepted 9 January 2016
Available online 2 February 2016

Keywords:
Hardness
Irradiation
Nix-Gao Model
Stainless Steel

ABSTRACT

Specimens of stainless steel reactor internals were irradiated with 240 keV protons and 6 MeV Xe ions at room temperature. Nanoindentation constant stiffness measurement tests were carried out to study the hardness variations. An irradiation hardening effect was observed in proton- and Xe-irradiated specimens and more irradiation damage causes a larger hardness increment. The Nix-Gao model was used to extract the bulk-equivalent hardness of irradiation-damaged region and critical indentation depth. A different hardening level under H and Xe irradiation was obtained and the discrepancies of displacement damage rate and ion species may be the probable reasons. It was observed that the hardness of Xe-irradiated specimens saturate at about 2 displacement/atom (dpa), whereas in the case of proton irradiation, the saturation hardness may be more than 7 dpa. This discrepancy may be due to the different damage distributions.

1. Introduction

Austenitic stainless steels are essential structural materials that are widely used in light-water reactor internals due to their excellent strength, ductility, and corrosion-resistance properties. The reliability and integrity of such stainless steel internals are of particular importance for the safe operation of reactors. Irradiation hardening has been a concern for reactor internals in radiation environments during long-term service, and is considered as an important reason for various phenomena, such as irradiation-assisted stress corrosion cracking [1]. Therefore, it is essential to understand the hardening behavior of stainless steel internals.

Because of the difficulties associated with conducting neutron irradiation studies, charged particles (protons and heavy ions) were chosen to simulate the irradiation hardening behaviors of neutron irradiation. However, compared with the nearly uniform distribution of neutron irradiation damage, the shallow penetration depth and nonuniform irradiation damage distribution by ions irradiation create difficulties for hardness results analysis. It is therefore critical to extract the bulk hardness at corresponding irradiation damage from the

* *Corresponding author.*
E-mail address: xuchaoliang@cgnpc.com.cn (C. Xu).
http://dx.doi.org/10.1016/j.net.2016.01.007

nonuniform damage distribution. Moreover, many researchers choose protons or heavy ions to study irradiated hardening, mainly due to their accelerated effects, which are regarded as advantageous. However, only a few studies have been carried out to investigate the mechanical properties under different ion (protons or heavy ions) irradiation, and little is known about any additional hardening effects caused by different damage rates. Therefore, before analyzing the effect of hardening, the first thing we should do is to clarify hardening behaviors by different ion irradiation.

In the past decades, the nanoindentation technique was used to investigate mechanical properties after ion irradiation. These nanoindentation hardness data are valuable for scientific discussion. Moreover, the nanoindentation hardness data can be converted into the macroscopic Vickers hardness using the methods developed by Takayama et al. [2] and Kang et al. [3] based on the equation:

$$H_0 = 0.01\mathrm{HV} + 0.025 \quad (1)$$

This method extends the discussion scope of nanoindentation hardness and can provide more references for engineering issues.

In this work, the irradiation hardening behaviors of the stainless steel reactor internals after proton and xenon irradiation were investigated by nanoindentation tests. The hardness of the ion-irradiated damage region was characterized by the Nix-Gao model. The hardening effect of protons and Xe ions irradiation was discussed and then the probable reason was given.

2. Materials and methods

The material used in this study was austenite stainless steel (Z6CND17.12) used for reactor baffle-former bolts. The specimens used in our experiments were cut from bars by solution treatment at 1,060 °C for 90 minutes, followed by air cooling. The chemical composition of this material is presented in Table 1.

The plate specimens ($10 \times 10 \times 1$ mm^3) were polished until they become mirror-like before irradiation. The specimens were irradiated with 240 keV protons and 6 MeV Xe^{26+} ions at room temperature in a chamber with a vacuum of 10^{-5} Pa at the ECR-320-kV High-Voltage Platform in the Institute of Modern Physics (Lanzhou, Gansu province). The specimens were irradiated to 5×10^{17} ions/cm^2, 1×10^{18} ions/cm^2, and 3.5×10^{18} ions/cm^2 with protons and 6.6×10^{14} ions/cm^2, 2.3×10^{15} ions/cm^2, and 5×10^{15} ions/cm^2 with Xe ions. According to the Monte Carlo code *SRIM 2012* [4], these fluences correspond to the peak damage levels of 1 displacement/atom (dpa), 2 dpa, and 7 dpa for proton irradiation and 2 dpa, 7 dpa, and 15 dpa for Xe irradiation (density of 7.8 g/cm^3 and threshold displacement energies of 40 eV for Fe, Cr, and Ni sublattices [5]), as shown in Fig. 1. In the SRIM calculation process, the vacancy file obtained by the Kinchin–Pease quick calculation model was used to calculate the displacement damage values. The displacement damage rate for H and Xe irradiation is about 1.1×10^{-4} dpa/s and 8.0×10^{-4} dpa/s, respectively.

Table 1 – Chemical composition of the stainless steel Z6CND17.12.

Elements[a]	C	Si	Co	P	S
Weight (%)	0.038	0.340	0.010	0.008	0.003
Elements	Cr	Ni	Cu	Mo	Mn
Weight (%)	17.28	11.65	0.46	2.49	1.24

[a] Balance of composition is Fe.

Nanoindentation measurements of the specimens were carried out using a diamond Berkovich indenter in a Nano Indenter G200 (Agilent Technologies) at Suzhou Institute of Nano-Tech and Nano-Bionics (Suzhou, Jiangsu province). The continuous stiffness measurement mode was chosen to obtain a hardness (H) versus depth (h) profile. The hardness was calibrated using a fused silica reference material to 2.0 μm depth. Specimens were mounted onto aluminum stubs with hot wax and indents were produced in a direction normal to the specimen surface. The maximum penetration depth and applied load were about 2.0 μm and 330 mN, respectively. Each specimen was tested five times at different points, and average values were taken for analysis. The distance between indentations was ~50 μm. Because of the deviation from the ideal shape of the diamond indenter tip geometry and the surface effect of the specimens, the data from the surface to 50 nm were not accurate. Therefore, we did not use the hardness data from the surface to 50 nm in this study.

3. Results and Discussion

Fig. 2 shows the hardness versus the penetration depth of unirradiated specimens, specimens irradiated to 1 dpa, 2 dpa, and 7 dpa by protons and 2 dpa, 7 dpa, and 15 dpa by Xe. It can be clearly seen that the hardness of both proton- and Xe-irradiated specimens is larger than that of unirradiated specimens. This indicates an irradiation-hardening phenomenon of stainless steel. The irradiation hardness is fluence dependent, and higher fluence causes a greater hardness increment. It is well-known that hardening of irradiated specimens is mainly due to the formation of irradiation defects. Previous studies have proved that more irradiation defects will be produced by higher irradiation fluence [6,7]. Thus, it is reasonable that more significant hardening appears in higher fluence specimens.

The gradual decrease of hardness curves with indenter depth from around 50 nm to 2,000 nm was observed, as shown in Fig. 2. This decrease is caused by the indenter size effect. This effect can be explained by the model developed by Nix-Gao based on the geometrically necessary dislocation theory [8]. Using the Nix-Gao model, the hardness–depth profile is expressed as:

$$H = H_0(1 + h^*/h)^{0.5} \quad (2)$$

where H_0 is the hardness at infinite depth (i.e., bulk hardness) and h^* is a characteristic length that depends on the material and shape of the indenter trip. According to this model, with the increases in indentation depth (h), the

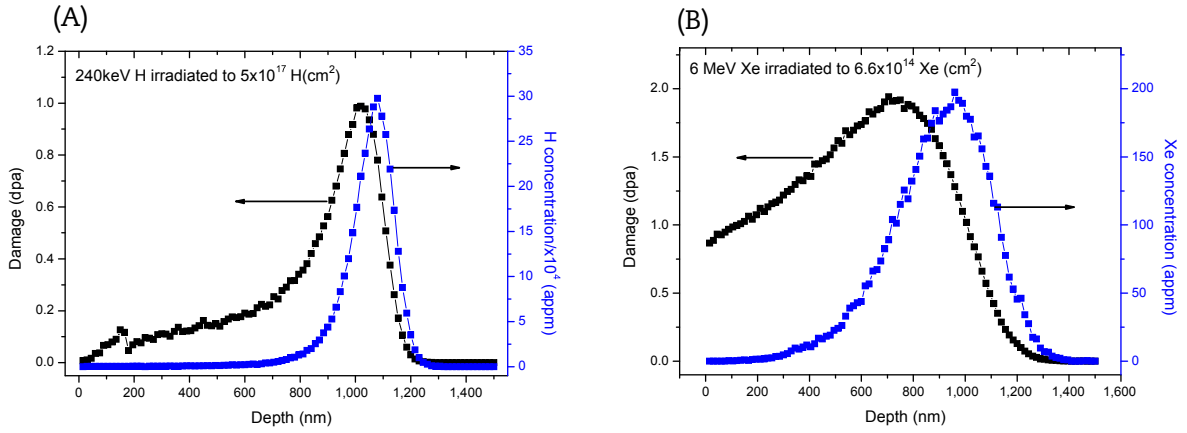

Fig. 1 – Distribution of displacement damage versus depth in irradiated stainless steel. (A) Stainless steel irradiated with 240 keV protons to 5 × 10^{17} ions/cm^2; and (B) stainless steel irradiated with 6 MeV Xe ions to 6.6 × 10^{14} ions/cm^2 according to simulation with SRIM 2012. dpa, displacement/atom.

measured hardness value decreases gradually and approaches H_0 progressively.

The measured hardness as a function of depth does not represent the actual hardness of the material at that depth. To obtain the real hardness of the irradiated layer, the Nix-Gao model has been used to evaluate irradiation hardening for ion-irradiated materials [9–11]. According to this method, the nanoindentation hardness data are plotted as H^2 versus 1/h, as shown in Figs. 3 and 4 for proton and Xe irradiation, respectively. It is observed that the unirradiated specimen has a good linearity above 50 nm. However, the irradiated specimens appear to have a bilinearity with an inflexion point at around 180–300 nm. As reported in previous studies [2], the bilinear behavior is due to the softer substrate effect of the unirradiated layer beneath the irradiated layer and the measured hardness is influenced by the softer substrate up to a critical depth, h_c. The inflexion point (critical depth h_c) is therefore regarded as the depth obtained using the actual bulk-equivalent hardness H_0 of the irradiated layer [9]. The bulk-equivalent hardness of the damaged layer H_0 can be obtained by fitting the curves from 50 nm to inflexion point, or simply from the intercept with the H^2 axis in the H^2 versus 1/h curves [8].

Table 2 shows the H_0 extrapolated from the hardness data for the unirradiated and irradiated specimens according to the Nix-Gao model. The critical indentation depth, h_c, is derived from the inflexion point of bilinear curves. As the results in Table 2 show, if taking into account the critical indentation depth of H^2–1/h curves, as the transition depth reflects the real hardness, it is noticed that the indentation depth at around 1/5 and 1/3 of the peak damage depth reflects the real hardness of the proton- and Xe-irradiated specimens. That is to say, with the Berkovich diamond indenter tip, the hardness at around 1/5–1/3 peak damage depth is regarded as an approximate value of ion-irradiated specimens. Previously, Samuels and Mulhearn [12] reported that the stress field from the indenter spread about seven times the contact depth. Huang et al. [10] suggested that the indenter tip extended down approximately six times the indenter's contact depth. Our previous hardness analysis of 16MND5 after Fe ions and proton irradiation indicated that the bulk hardness of the

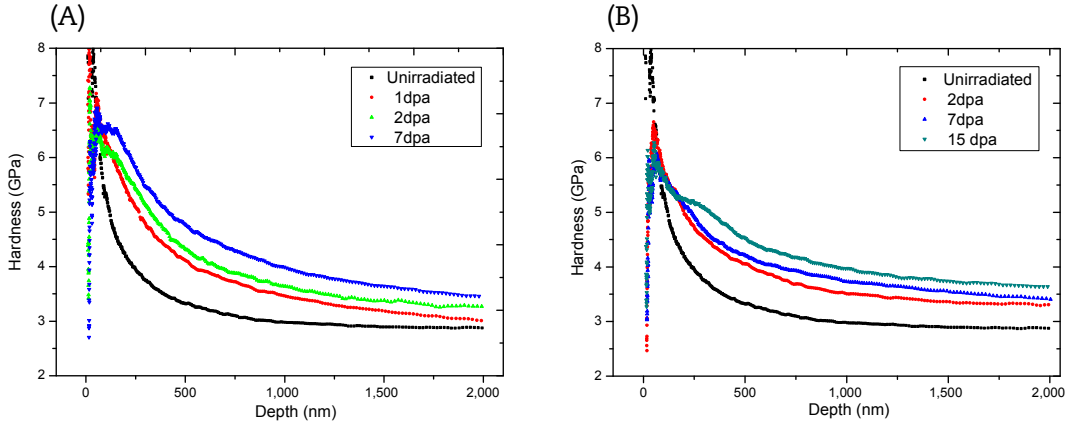

Fig. 2 – Hardness versus penetration depth in unirradiated and irradiated stainless steel with different fluences. (A) Unirradiated and proton-irradiated stainless steel; and (B) unirradiated and Xe-irradiated stainless steel with different fluences. dpa, displacement/atom.

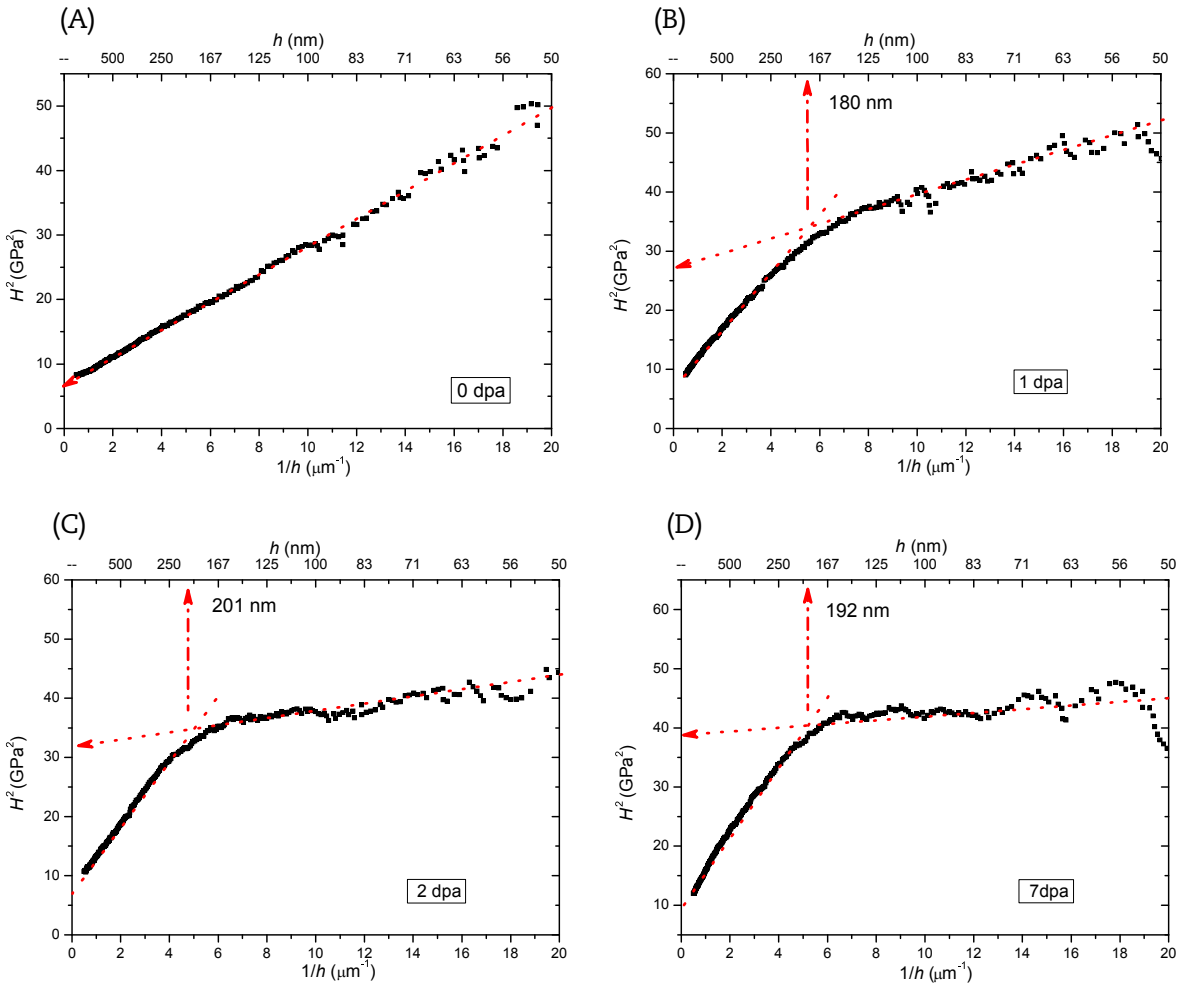

Fig. 3 – Curves of H^2 versus 1/h for average hardness of stainless steel by proton irradiation. Proton irradiation to (A) 0 dpa, (B) 1 dpa, (C) 2 dpa, and (D) 7 dpa. dpa, displacement/atom.

irradiated layer calculated from the Nix-Gao model can be obtained at about 1/5 of the peak damage depth [13]. The results based here on the Nix-Gao model are close to these previously reported results.

It should be noted that the h_c increases with the damage level for Xe-irradiated specimens, but it is around 190 nm for proton-irradiated specimens. Kasada et al. [9] pointed out that the h_c depends on the irradiation hardening level of an ion-irradiated surface. Therefore, considering the different ion irradiation damage distribution at the surface area shown in Fig. 1, it can be concluded that there exists a different hardening effect caused by proton and Xe irradiation. This may cause a different critical depth h_c. However, this is only one possible explanation, and more studies are needed to obtain in-depth information about h_c.

Fig. 5 shows variations of the H_0 obtained from the Nix-Gao model, with irradiation damage caused by proton and Xe ions. It is observed that the hardness of H-irradiated specimens is significantly higher than that of Xe-irradiated specimens at the same displacement damage level. The primary difference between these two types of ion irradiation is the damage rate [a higher damage rate of Xe irradiation (8.0×10^{-4} dpa/s) and a lower damage rate of proton irradiation (1.1×10^{-4} dpa/s)] and ion species. Thus, the differences in damage rate and ion species may be the main reasons for this hardness discrepancy at equivalent damage levels.

Our previous studies on 16MND5 steel irradiated by Fe ions (3×10^{-4} dpa/s) and proton (1×10^{-4} dpa/s) suggest that the lower-damage rate irradiation will cause a relatively higher increase in hardness [13]. Hardie et al. [14] also indicated that Fe–Cr alloys irradiated with a relatively lower fluence rate will induce the irradiation hardening phenomenon more significantly. It is known that the introduction and evolution of defects are the root cause of hardness variations. The lower damage rate results in a lower density of defects/unit time and interaction between radiation-induced defects will occur less frequently [14]. Thus, the fraction of surviving point defects or simple defects is higher and the nucleation rate of defect clusters is lower at lower damage rates because the absolute of point defect flux to sinks is lower. In fact, Hardie et al. [14] have indicated that a lower dislocation density was introduced at a low damage rate than at a high damage rate. Lee et al. [15] also proved that a lower damage rate was less effective in producing defects such as black dots and dislocation loops at equivalent damage. Thus, due to a high density of simple defects, which will pin dislocation effectively under

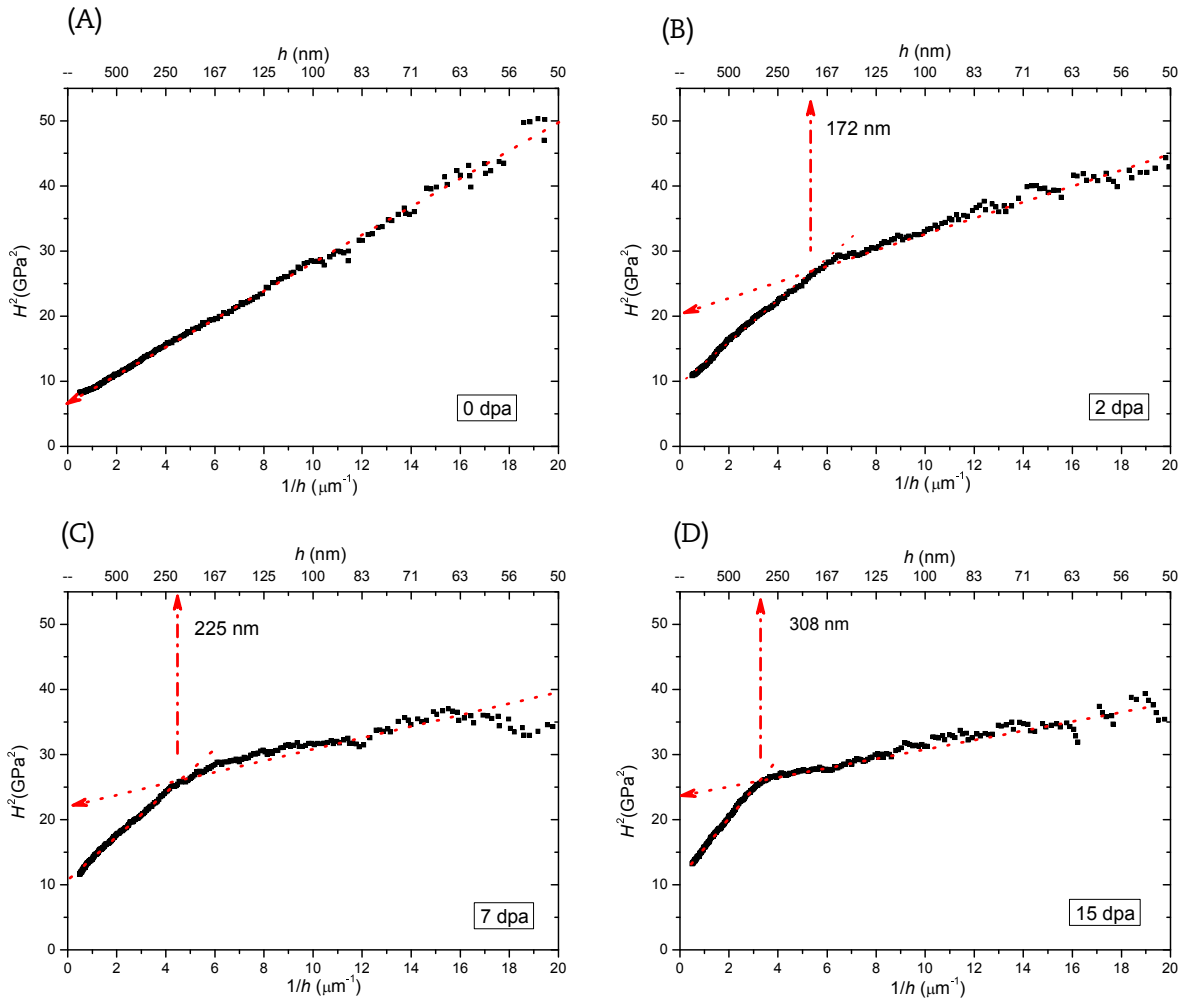

Fig. 4 – Curves of H^2 versus 1/h for average hardness of stainless steel by Xe irradiation. Xe irradiation to (A) 0 dpa, (B) 2 dpa, (C) 7 dpa, and (D) 15 dpa. dpa, displacement/atom.

a low damage rate, the hardness of proton-irradiated specimens will show a higher hardness increment compared with the Xe-irradiated specimens.

Moreover, we cannot neglect the role of irradiation ion species in determining hardness. Previous studies have indicated that the H irradiation will form H bubbles or H/vacancy easily due to its high migration rate and the density of H bubbles or H/vacancy depends on the H concentration. Similar results can be found with other lighter gas ions irradiation by transmission electron microscopy (TEM) observation [16]. Therefore, the implantation to nearly 3×10^5 appm/dpa in the case of proton irradiation at maximum concentration depth will produce a high concentration of H/vacancy complexes or gas bubbles, which would provide a stronger barrier to the dislocation motion, and therefore cause an additional hardening [17]. While in the case of Xe irradiation, according to previous TEM studies [18], a low concentration of 100 appm/dpa will not introduce obvious gas bubbles compared with proton irradiation. In fact, Yun et al. [19] indicated that the fluence level of Xe bubbles formation was above 1.1×10^{16} ions/cm^2. This fluence is two times higher than the fluence we used. Thus, compared with Xe irradiation, a higher concentration of H ions at the same displacement damage level is another reason for the higher hardness increment.

It is known that the irradiation hardening of austenitic stainless steel saturates at a few displacement/atom values [11,20]. In our case, the different saturation hardness can be obtained for proton and Xe irradiation. As observed in Fig. 5, the hardness of Xe-irradiated specimens was saturated at 2 dpa, whereas in the case of proton irradiation, the saturation

Table 2 – The H_0 obtained from the Nix-Gao model and the corresponding critical indentation depth h_c in the hardness–depth curve.

	Peak damage depth (nm)	Damage (dpa)	H_0 (Gpa)	h_c (nm)
Unirradiated	–	0	2.7	–
H irradiated	1,020	1	5.2	180
		2	5.7	201
		7	6.2	192
Xe irradiated	750	2	4.5	187
		7	4.7	225
		15	4.8	308

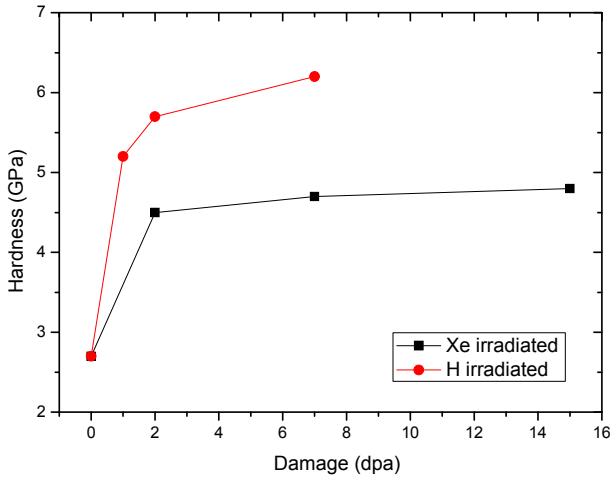

Fig. 5 – H_0 obtained from the Nix-Gao model of specimens irradiated to different fluences by proton and Xe. dpa, displacement/atom.

hardness may be more than 7 dpa. This indicates that the saturation hardness decreases with the irradiation ions mass, increasing for H and Xe irradiation. In fact, Hunn et al. [21] analyzed He- and Fe-irradiated 316 stainless steel and suggested that the saturation hardness of He and Fe irradiation was around 10 dpa and 1 dpa, respectively. Therefore, we can conclude that the saturation hardness of ion-irradiated stainless steel is a function of irradiation ion species. Hardness saturation begins first at more heavy irradiation ions. It seems that the heavier the irradiation ion mass used, the lower the saturation hardness obtained under our irradiation conditions.

Hardness variations caused by H and Xe irradiation are closely related to the irradiation damage. Irradiation of Xe ions produces a near-uniform distribution of atomic displacement damage (the ratio of minimum and maximum damage is about 50% from the surface to peak damage region), whereas protons produce a remarkable nonuniform distribution of displacement damage with a steep peak at the end of the projective range, as shown in Fig. 1. If the average damage level (over the whole projective ranges of ion-damaged layer) is used instead of the peak damage level, the average damage level of Xe irradiation is close to the peak damage level, but a large distinction between the average damage and peak damage levels of proton irradiation indeed exists. Therefore, to obtain a similar average damage of the irradiation region to a heavier ion irradiation, more irradiation fluence (damage) is needed for lighter ion irradiation. That is to say, although the saturation fluence of H irradiation is higher, the average damage level of the damage region is actually much lower.

In a summary, nanohardness tests were used to investigate the mechanical properties of stainless steel reactor internals irradiated by 240 keV protons and 6 MeV Xe ions at room temperature. Ion irradiation causes a remarkable hardening effect in both proton- and Xe-irradiated specimens and more irradiation damage causes a higher hardness increment. The bulk-equivalent hardness of irradiation-damaged layer is deduced from the Nix-Gao model and can be obtained from the hardness around 1/5–1/3 of the peak damage depth. The hardness irradiated with H is higher than that with Xe at the same damage level due to the difference in the irradiation damage rate and ion species. The saturation hardness of H irradiation is larger than that of Xe irradiation and the different damage distribution may be the primary reason.

Conflicts of interest

All contributing authors declare no conflicts of interest.

Acknowledgments

The authors would like to thank the 320-kV High-Voltage Platform in Institute of Modern Physics for ion irradiation experiments.

REFERENCES

[1] G.S. Was, Fundamentals of Radiation Materials Science: Metals and Alloys, Springer, New York, 2007.
[2] Y. Takayama, R. Kasada, Y. Sakamoto, K. Yabuuchi, A. Kimura, M. Ando, D. Hamaguchi, Nanoindentation hardness and its extrapolation to bulk-equivalent hardness of F82H steels after single- and dual-ion beam irradiation, J. Nucl. Mater. 442 (2013) S23–S27.
[3] S.K. Kang, J.Y. Kim, C.P. Park, H.U. Kim, D. Kwon, Conventional Vickers and true instrumented indentation hardness determined by instrumented indentation tests, J. Mater. Res. 25 (2010) 337–343.
[4] J.P. Biersack, L.G. Haggmark, A Monte Carlo computer program for the transport of energetic ions in amorphous targets, Nucl. Instrum. Methods 174 (1980) 257–269.
[5] ASTM, Standard Practice for Neutron Radiation Damage Simulation by Charged-particle Irradiation (ASTM 521-96), West Conshohocken, PA, 2003.
[6] R.D. Carter, D.L. Damcott, M. Atzmon, G.S. Was, E.A. Kenik, Effects of proton irradiation on the microstructure and microchemistry of type 304L stainless steel, J. Nucl. Mater. 205 (1993) 361–373.
[7] G. Gupta, Z. Jiao, A.N. Ham, J.T. Busby, G.S. Was, Microstructural evolution of proton irradiated T91, J. Nucl. Mater. 351 (2006) 162–173.
[8] W.D. Nix, H. Gao, Indentation size effects in crystalline materials: a law for strain gradient plasticity, J. Mech. Phys. Solids 46 (1998) 411–425.
[9] R. Kasada, Y. Takayama, K. Yabuuchi, A. Kimura, A new approach to evaluate irradiation hadening of ion-irradiated ferritic alloys by nano-indentation techniques, Fusion Eng. Des. 86 (2011) 2658–2661.
[10] H.F. Huang, D.H. Li, J.J. Li, R.D. Liu, G.H. Lei, Nanostructure variations and their effects on mechanical strength of Ni–17Mo–7Cr alloy under xenon ion irradiation, Mater. Transact. 55 (2014) 1243–1247.
[11] K. Yabuuchi, Y. Kuribayashi, S. Nogami, R. Kasada, A. Hasegawa, Evaluation of irradiation hardening of proton irradiated stainless steels by nanoindentation, J. Nucl. Mater. 446 (2014) 142–147.

[12] L.E. Samuels, T.O. Mulhearn, An experimental investigation of the deformed zone associated with indentation hardness impressions, J. Mech. Phys. Solids 5 (1957) 125–134.
[13] X. Liu, R. Wang, A. Ren, J. Jiang, C. Xu, P. Huang, W. Qian, Y. Wu, C. Zhang, Evaluation of radiation hardening in ion-irradiated Fe based alloys by nanoindentation, J. Nucl. Mater. 444 (2014) 1–6.
[14] C.D. Hardie, C.A. Williams, S. Xu, S.G. Roberts, Effects of irradiation temperature and dose rate on the mechanical properties of self-ion implanted Fe and Fe–Cr alloys, J. Nucl. Mater. 439 (2013) 33–40.
[15] E.H. Lee, J.D. Hunn, T.S. Byun, L.K. Mansur, Effects of helium on radiation-induced defect microstructure in austenitic stainless steel, J. Nucl. Mater. 280 (2000) 18–24.
[16] I.I. Chernov, A.N. Kalashnikov, B.A. Kalin, S. Yu, Binyukova, Gas bubbles evolution peculiarities in ferritic–martensitic and austenitic steels and alloys under helium-ion irradiation, J. Nucl. Mater. 323 (2003) 341–345.
[17] H. Zhang, C. Zhang, Y. Yang, Y. Meng, J. Jang, A. Kimura, Irradiation hardening of ODS ferritic steels under helium implantation and heavy-ion irradiation, J. Nucl. Mater. 455 (2014) 349–353.
[18] M. Chai, W. Lai, Z. Li, W. Feng, Radiation damage of 1Cr18Ni9Ti and Zr-Ti-Al alloys due to energetic particle irradiation, Acta Metall. Sin. (Engl. Lett.) 25 (2012) 29–39.
[19] D. Yun, M.A. Kirk, P.M. Baldo, J. Rest, A.M. Yacout, Z.Z. Insepov, *In situ* TEM investigation of Xe ion irradiation induced defects and bubbles in pure molybdenum single crystal, J. Nucl. Mater. 437 (2013) 240–249.
[20] G.R. Odette, G.E. Lucas, The effects of intermediate temperature irradiation on the mechanical behavior of 300-series austenitic stainless steels, J. Nucl. Mater. 179–181 (1991) 572–576.
[21] J.D. Hunn, E.H. Lee, T.S. Byun, L.K. Mansur, Helium and hydrogen induced hardening in 316LN stainless steel, J. Nucl. Mater. 282 (2000) 131–136.